Role of Isomerization Barriers in the pK_a Control of the Retinal Schiff Base: A Density Functional Study

Emadeddin Tajkhorshid, Béla Paizs, and Sándor Suhai*

Department of Molecular Biophysics, German Cancer Research Center, Im Neuenheimer Feld 280, D-69120 Heidelberg, Germany

Received: June 15, 1998; In Final Form: March 4, 1999

The barriers to the rotation of all conventional single and double bonds have been calculated in a model Schiff base which is structurally very close to the retinal Schiff base chromophore in bacteriorhodopsin (bR). The calculated values for the torsional barriers can be used, therefore, to estimate the corresponding values in the retinal Schiff base structure. The torsional barriers are calculated as the energy differences between the all-trans and 90°-rotated conformers, respectively, for optimized structures in both neutral and protonated species. To study the effect of the isomerization on the pK_a of the Schiff base, for each 90°-rotated conformer the gas-phase proton affinity of the system has also been calculated and compared with the proton affinity of the all-trans conformer. The results clearly show that protonation of the nitrogen in the Schiff base group has a profound effect on the barriers to the rotation around different bonds in the system. For 90°-twisted species, completely different mesomeric structures are predicted for single or double bond rotations as well as for the protonated and the neutral species. The C═N double bond and the double bond next to the Schiff base group in the protonated Schiff base (corresponding to the C_{13}═C_{14} bond of the retinal Schiff base in the bR which is assumed to rotate during the photoisomerization) have the lowest isomerization barriers among the double bonds. In the neutral species, however, high barriers to these rotations are predicted. The proton affinity of the system decreases upon the isomerization around the single bonds, while the rotation around the double bonds significantly increases the calculated values for the proton affinities. This may be considered as one of the possible mechanisms by which the protein environment controls the pK_a of the retinal Schiff base chromophore. The predicted low barrier to the C_{13}═C_{14} double bond rotation is needed for the ground-state isomerization of the chromophore in the last step of the bR photocycle and also in the dark adaptation of the pigment. Protonation of the retinal Schiff base chromophore, therefore, seems to be a prerequisite for these ground-state isomerization events in bR.

1. Introduction

The transmembrane protein bacteriorhodopsin (bR) present in the outer purple membrane of *Halobacterium salinarium* (formerly *H. halobium*) is one of the simplest known active membrane transport systems. It functions as a light-driven proton pump converting light energy into a proton gradient which is used by the cell as an energy source to activate ATP synthase. Structurally, it folds into seven transmembrane helices, one of them containing the residue Lys_{216} at which the retinal prosthetic group binds via a protonated Schiff base linkage (for reviews see refs 1−5). The chromophore divides the channel formed by the α-helices of the polypeptide into a cytoplasmic part connecting to the inside of the cell and an extracellular part connecting to the outside.

The general features of the transport mechanism are now understood. The absorption of a photon which starts the bR photocycle induces an excited state of the chromophore followed by the isomerization of the retinal protonated Schiff base around the C_{13}═C_{14} double bond next to the Schiff base group. During the photocycle of bR, the initially protonated retinal Schiff base releases a proton into the extracellular part of the channel and will be reprotonated from a proton source located in the cytoplasmic part. Therefore, a proton is effectively pumped from the inside of the cell to the outside during each cycle.[1−5] There are, however, different proposals regarding when and how the proton starts to move from the retinal Schiff base to the next proton accepting group which is suggested to be the negatively charged carboxylate group of Asp_{85} in the protein backbone.[3] This proton transfer from the protonated Schiff base to the Asp_{85} side chain can be mediated by one or two water molecule(s) present in the vicinity of the chromophore.

The involvement of water molecules in the stability of the protonated Schiff base was suggested by DuPuis et al.[6] and by Hildebrandt and Stockburger[7] on the basis of the resonance Raman study of dried membranes. The presence of water in the binding site was shown by de Groot et al.[8] on the basis of the ^{15}N NMR studies. Recent crystal structures of bR also demonstrate the presence of a few water molecules in the vicinity of the Schiff base group.[9,10] The effect of the water molecules on the pK_a of the Schiff base group is demonstrated by pK_a measurement of a series of retinal Schiff base analogues.[11] The possible positions of hydrogen-bonded water molecules around the Schiff base group have been theoretically examined.[12,13]

The proton transport mechanism in bR is based on the sequential changes in the pK_a values of the retinal Schiff base and vectorially arranged protonatable groups in the protein. The pK_a change of respective groups in the proton channel, especially the pK_a of the retinal Schiff base, plays a crucial role in the

* To whom all correspondence should be addressed. Tel: +49 6221 42 2369. Fax: +49 6221 42 2333. E-mail: S.Suhai@DKFZ-Heidelberg.de.

10.1021/jp982625d CCC: $18.00
Published on Web 05/01/1999

proton-transfer reaction. There are several possible reasons explaining why the pK_a of the Schiff base would be lowered at the beginning of the deprotonation step. Among these are the disruption of the π-system of the retinal Schiff base chain during the trans-to-cis isomerization, which decreases the electronic density on the nitrogen atom of the Schiff base group,[14,15] and the conformational changes which modify the electrostatic environment of the retinal Schiff base[16,17,18] or change the orientation of the hydrogen-bonded groups.[19,20] The decrease in the pK_a of the Schiff base is the first step which may induce the proton transfer. It should be mentioned, however, that the pK_a of the retinal Schiff base will be significantly increased in the protein environment as compared with its isolated form. It is known from experimental data that the pK_a of the protonated retinal Schiff base in methanol/water (1:1) solution is about 7.2[21,22] while the pK_a of the chromophore in bR is shifted to 13.3.[23,24] The protein environment seems to have a very strong effect on the pK_a of the retinal Schiff base. With regard to this, the presence of the negatively charged side chains of Asp_{85} and Asp_{212} in the vicinity of the protonated Schiff base is proposed to have the main influence on the electronic structure and charge distribution of the retinal Schiff base in the bR protein environment.[25]

The dynamics of the excited state of the retinal in bR and the effect of the protein environment on the rate of its photoisomerization have been experimentally investigated.[26−29] The dynamics of the all-trans and the 13-cis conformers of the retinal protonated Schiff base has also been studied recently in different solvents by means of picosecond transient spectroscopy.[30] Ab initio molecular dynamics calculations on all-trans and 11-cis retinal[31] have been reported recently, and combined QM/MM dynamics simulations have been performed in order to understand the photoisomerization process of bR.[32] The dynamic behavior of the retinal Schiff base structure in different stages of the bR photocycle has been theoretically studied using classical force fields[33−39] or combined classical and quantum chemical approaches where ab initio techniques have been applied to calculate the electronic characteristics of the retinal Schiff base structures, obtained from classical molecular dynamics simulation of bR.[40] In agreement with very first semiempirical simulations of the excited-state potential energy surfaces,[41−43] there are very recent papers investigating ab initio photoisomerization dynamics of different retinal chromophore models.[44,45,46]

In this paper we will present the barriers to the rotation of different double bonds and single bonds of a model Schiff base. The isomerization barriers will be presented for both protonated and unprotonated species of the molecule. The torsional barriers will be computed on the basis of the relative energies of the all-trans and 90°-rotated species for the optimized structures in both neutral and protonated species calculated at the spin-restricted and spin-unrestricted Becke3LYP density functional levels of theory and using 6-31G and 6-31G* basis sets. To study the potential effect of the isomerization on the pK_a of the Schiff base, at each 90°-rotated geometry the gas-phase proton affinity (PA) of the system has also been calculated. The obtained results will be discussed on the basis of the atomic charges, bond alternation, and different mesomeric structures presented for planar and 90°-rotated species of the protonated and unprotonated Schiff base molecules.

2. Computational Details

For the computer graphics and the initial construction of the molecular models we used the InsightII software[47] running on a Silicon Graphics Indigo2 workstation. The model Schiff base was considered as neutral and protonated species, respectively. Gradient optimization techniques were employed to optimize the geometry of the molecules at the DFT level, using 6-31G and 6-31G* basis sets, respectively. Except for the constrains used for the 90°-rotated species, optimizations were performed without any geometric restrictions and using the default GAUSSIAN 94 [48] convergence criteria. The hybrid Becke3LYP (B3LYP) method was used for the DFT calculations. In every set of the geometry optimizations of the 90°-rotated species the same geometry constrains were applied for the neutral and protonated model Schiff base molecules. All ab initio calculations were performed with the GAUSSIAN 94 [48] implementation of DFT on an IBM SP2 cluster.

During the spin-unrestricted calculations we have mixed the highest occupied initial guess orbital with the lowest unoccupied one in order to destroy the closed shell nature of the initial guess. Whenever a lower energy unrestricted Becke3LYP (UB3LYP) solution was found, the geometry was reoptimized by the UB3LYP model as well.

The gas-phase proton affinity (PA) of a compound B can be calculated as the negative standard reaction enthalpy of protonation at 298.15 K:

$$B + H^+ \rightarrow BH^+$$

$$PA = -[E_{DFT}(BH^+) - E_{DFT}(B) + (E_{vib}(BH^+) - E_{vib}(B))] + \frac{5}{2}RT$$

Here E_{DFT} will be obtained from the DFT calculations, E_{vib} includes the zero point energy and temperature corrections to the vibrational enthalpy, and $^5/_2RT$ includes the translational energy of the proton and the $\Delta(PV)$ term. It is shown that the inclusion of the zero point energies does not have any significant effect on the relative PA values in different Schiff base models.[49,50] Because of the comparative nature of the study and because of the cost of the calculations, E_{vib} terms are not considered in the calculation of the PA values.

It has been shown that the length of the conjugated double bonds has a significant effect on the PA of the system.[49] For this reason the retinal Schiff base was approximated to a conjugated Schiff base including six conjugated double bonds in the present study.

The atomic charges were derived from a Mulliken population analysis, as implemented in the GAUSSIAN 94 program. The atomic charge reported for each heavy atom includes the charges of the connected hydrogen(s) to it.

In the 90°-rotated species the molecule can be considered as consisting of two isolated π-electronic subsystems which do not have any $\pi-\pi$ interaction with each other. For simplifying the discussion, we refer to the nitrogen containing moiety and the other part of the molecule as N-part and C-part, respectively.

3. Results and Discussion

3.1. Model Description. The structure of the all-trans protonated retinal Schiff base which is proposed to be the starting configuration of the chromophore at the beginning of the bR photocycle and its conventional atom numbering are depicted in Figure 1. The structure of the model Schiff base which was used to represent the retinal Schiff base in the present study is also shown in Figure 1. The atom numbering (N_1 to C_{12}) and the bond numbering (B_1 to B_{11}) used in the present study for the model Schiff base structure start from the nitrogen atom and its double bond, respectively, and continue toward

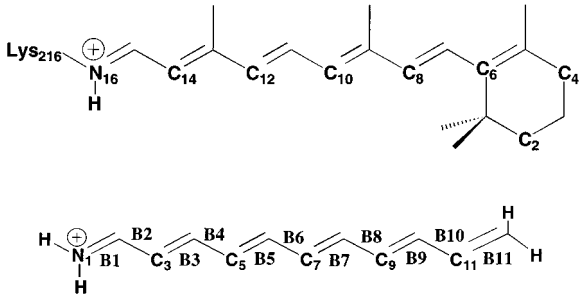

Figure 1. Retinal Schiff base structure in the ground state of the bR photocycle and its conventional numbering scheme (top). Atom and bond numbering used in the text in the case of the all-trans structure of the model Schiff base with six conjugated double bonds (PSB) (bottom).

the other end of the chain. The results obtained from the calculations performed on different conjugated Schiff base structures have shown that, compared to the effect of the number of the double bonds conjugated to the Schiff base group (C═N), the presence of the methyl groups on the main chain or the alkylation of the nitrogen atom has much less effect on the extent of the π-electron delocalization of the system.[49] The location of the methyl groups on the polyene side chain is, however, of utmost importance in determining the overall shape of the retinal analogues used as ligands for bR during experiments.[51] These structural effects, added to the dominant steric and electronic restrictions of the binding pocket,[26,27] would explain the discrimination exhibited by the protein binding site for different analogues during incubation studies.[51] Such effects can also influence the rate of the photoisomerization and the dynamics of the ground and excited states of the retinal Schiff base.[26−29] The importance of the methyl groups has also been discussed during the study of the excited-state potential energy surface of the isomerization in different isomers of the retinal.[52,53] We also believe that the methyl substitutions can significantly influence the PA values and the barriers against the rotation of the double bonds.[50] In the present study, however, the model Schiff base will be treated as an isolated system and without inclusion of the protein environment, and we try to understand the trend of the effect of the rotation of different bonds on the PA of the model Schiff base. Therefore, for the sake of computer time, the methyl groups will not be considered in the model.

A ring-chain s-trans planar conformation adopted by the retinal chromophore in the bR binding pocket, rather than the twisted s-cis conformation energetically favored in solution, has been experimentally shown. The planarity of ring-chain was first suggested by Schreckenbach.[54] The s-trans conformation was deduced from ^{13}C NMR chemical shifts of bR by Mathies and Griffin[55] and supported by studies with locked *s-cis*- and *s-trans*-retinal which were incorporated into bR.[56] For the all-trans conformer, both the ab initio calculations[49,57] and the experimental crystallographic studies[58] demonstrate a planar structure. Therefore, to model the chromophore in bR, a Schiff base with six conjugated double bonds was selected. The results of our previous study clearly showed that the length of the conjugated double bond system has a significant effect on the electronic structure, the atomic charges, and the PA values of the protonated Schiff bases.[49] Therefore, we kept the complete conjugated double bonds in the model applied for the calculations.

Density functional theory (DFT) has been used in the calculation of the potential energy surface of the isomerization of both single and double bonds for very similar structures.[49,59,60] It has been reported that the results are in a good agreement with other methodologies applying higher levels of theory with respect to the description of the 90°-rotated species in the double bond rotations as well as the single bond rotations. The results from DFT spin-unrestricted calculations reasonably describe the 90°-rotated structures which will be formed during the rotation of the double bonds. The applicability of DFT in the calculation of the isomerization barriers and the description of the transition states of such rotations has been reported for neutral polyene systems such as β-carotene analogues.[60]

DFT techniques have also been used for studying the conjugated Schiff base structures, and the ability of DFT calculations in description of the 90°-rotated species are comparable with CAS−SCF level of theory calculations.[49,59] However, it seems that when the π-electronic system under study is significantly polarized, DFT calculations result in an overestimated π-electron delocalization effect. The results from the DFT calculations on the retinal (containing a carbonyl group as the terminal group), for example, predict a smaller bond alternation for the planar structure of the molecule[31] as compared to the experimental values.

For the conjugated Schiff base structures, the calculations carried out using a multireference wave function predict a larger bond alternation for both neutral[59] and protonated species,[45,46,59] as compared to the DFT results (see ref 59 for detailed comparison). The difference is more significant for the protonated species. In the B3LYP/6-31G* optimized structure of a conjugated Schiff base model with four double bonds, for example, the bond distances of B_1 (N_1═C_2) and B_3 (C_3═C_4) double bonds of the all-trans conformer are 1.323 and 1.385 Å, respectively.[49] The corresponding bond lengths are 1.293 and 1.362 Å, respectively, according to the CAS−SCF calculations applying eight electrons and eight orbitals in the active space.[59] For the single bonds, on the other hand, DFT results in shorter bond distances. The B_2 (C_2−C_3) and B_4 (C_4−C_5) single bonds, for example, are calculated to be 1.398 and 1.412 Å, respectively, according to the DFT results,[49] whereas the CAS−SCF calculations predict the values of 1.423 and 1.439 Å, respectively, for these bonds.

Because of the larger bond alternation in CAS−SCF calculations, the isomerization barriers calculated for the single bonds and the double bonds are respectively smaller and larger than the corresponding values in DFT calculations. The barrier against the rotation of the B_3 double bond (in a Schiff base model with four conjugated double bonds) calculated using CAS−SCF calculations are 43.2 and 47.3 kcal/mol, respectively, for protonated and neutral species. According to the DFT results, the corresponding values for the barrier against this rotation in the protonated and neutral species are 39.0 and 42.0 kcal/mol, respectively. This point has to be kept in mind whenever the absolute values for the barriers, which are calculated using DFT calculation in the present paper, are considered.

The lowering effect of the protonation on the double bond isomerization barriers and the consequent effect on the PA of the molecule, however, have the same trends in DFT and CAS−SCF calculations. In the above example, energetic comparison shows that the increase of the PA change of the molecule during the rotation of the B3 double bond is even slightly larger for the CAS−SCF calculations (4.0 kcal/mol),[59] as compared to the DFT results (3.0 kcal/mol). Therefore, despite the differences in the absolute values of the rotational barriers, it seems that the effect of the protonation on the barriers and the PA changes during the isomerizations are appropriately predicted using DFT calculations.

3.2. Isomerization Barriers. In the present study, using DFT calculations, we have calculated the barriers to the rotation of

TABLE 1: Bond Distances (Å) Calculated for the All-Trans and Different 90°-Rotated Species of the Neutral Model Schiff Base

	bond distances[a]										
	B_1	B_2	B_3	B_4	B_5	B_6	B_7	B_8	B_9	B_{10}	B_{11}
all-trans	1.2842	1.4521	1.3559	1.4372	1.3610	1.4347	1.3612	1.4366	1.3578	1.4463	1.3446
B1-90 (R)	**1.2918**	1.4551	1.3625	1.4312	1.3643	1.4318	1.3628	1.4352	1.3585	1.4458	1.3448
B2-90 (R)	1.2748	**1.4878**	1.3467	1.4454	1.3575	1.4375	1.3598	1.4378	1.3573	1.4467	1.3445
B3-90 (U)	1.3158	1.4083	**1.4720**	1.3602	1.4292	1.3829	1.4034	1.4056	1.3808	1.4324	1.3533
B4-90 (R)	1.2803	1.4619	1.3431	**1.4800**	1.3481	1.4462	1.3562	1.4405	1.3559	1.4476	1.3441
B5-90 (U)	1.2989	1.4285	1.4047	1.3767	**1.4757**	1.3638	1.4235	1.3933	1.3909	1.4267	1.3571
B6-90 (R)	1.2827	1.4554	1.3508	1.4492	1.3471	**1.4802**	1.3473	1.4486	1.3526	1.4497	1.3432
B7-90 (U)	1.2930	1.4376	1.3843	1.3982	1.4205	1.3659	**1.4760**	1.3719	1.4120	1.4156	1.3646
B8-90 (R)	1.2836	1.4534	1.3539	1.4412	1.3558	1.4464	1.3483	**1.4805**	1.3447	1.4564	1.3408
B9-90 (U)	1.2902	1.4421	1.3751	1.4101	1.4001	1.3856	1.4276	1.3612	**1.4748**	1.3935	1.3836
B10-90 (R)	1.2841	1.4525	1.3553	1.4384	1.3595	1.4376	1.3575	1.4453	1.3484	**1.4831**	1.3345

[a] The rotated bond is shown by the bold presentation of its distance. For the bond and atom numbering refer to Figure 1. The data are derived from the calculations at the restricted B3LYP/6-31G* level of theory except when there was an unrestricted solution with lower energy. In these cases the unrestricted B3LYP/6-31G* bond distances are reported. U and R stand for unrestricted and restricted B3LYP/6-31G* calculations, respectively.

TABLE 2: Bond Distances (Å) Calculated for the All-Trans and Different 90°-Twisted Species of the Protonated Model Schiff Base

	bond distances[a]										
	B_1	B_2	B_3	B_4	B_5	B_6	B_7	B_8	B_9	B_{10}	B_{11}
all-trans	1.3318	1.3876	1.3962	1.3976	1.3891	1.4069	1.3804	1.4182	1.3694	1.4370	1.3488
B1-90 (R)	**1.3926**	1.3622	1.4244	1.3806	1.4047	1.3953	1.3904	1.4100	1.3757	1.4324	1.3515
B2-90 (R)	1.2946	**1.4534**	1.3647	1.4253	1.3701	1.4234	1.3686	1.4286	1.2623	1.4425	1.3459
B3-90 (R)	1.3716	1.3497	**1.4691**	1.3680	1.4177	1.3888	1.3953	1.4067	1.3781	1.4307	1.3525
B4-90 (R)	1.3095	1.4163	1.3650	**1.4656**	1.3535	1.4390	1.3602	1.4355	1.3583	1.4454	1.3445
B5-90 (R)	1.3514	1.3664	1.4315	1.3573	**1.4659**	1.3720	1.4117	1.3980	1.3843	1.4271	1.3545
B6-90 (R)	1.3192	1.4013	1.3801	1.4220	1.3633	**1.4703**	1.3496	1.4453	1.3540	1.4482	1.3432
B7-90 (U)	1.3381	1.3836	1.4090	1.3811	1.4254	1.3630	**1.4700**	1.3724	1.4093	1.4149	1.3630
B8-90 (R)	1.3251	1.3943	1.3883	1.4076	1.3776	1.4266	1.3601	**1.4736**	1.3453	1.4554	1.3404
B9-90 (U)	1.3321	1.3907	1.3974	1.3960	1.4012	1.3883	1.4199	1.3677	**1.4692**	1.3929	1.3831
B10-90 (R)	1.3294	1.3899	1.3935	1.4008	1.3854	1.4123	1.3742	1.4302	1.3570	**1.4782**	1.3339

[a] The rotated bond is shown by the bold presentation of its distance. For the bond and atom numbering refer to Figure 1. The data are derived from the calculations at the restricted B3LYP/6-31G* level of theory except when there was an unrestricted solution with lower energy. In these cases the unrestricted B3LYP/6-31G* bond distances are reported. U and R stand for unrestricted and restricted B3LYP/6-31G* calculations, respectively.

all of the conventional single and double bonds in a model Schiff base structure which is structurally very close to the retinal Schiff base. Results from our previous study[49] showed that the most important parts of the retinal structure are in these kinds of studies the conjugated double bonds which can significantly influence the electronic properties of the Schiff base (C═N) group. Therefore, we performed our calculations on a model Schiff base structure which contains six conjugated double bonds (including the Schiff base group).

3.2.1. Protonated Schiff Base. The protonation has a profound effect on the conjugated electronic structure of the studied model Schiff base and significantly influences both the charge distribution and the bond alternation of the conjugated system. Comparison of the structures of the neutral and protonated species of the model Schiff base shows that the pattern of alternating short and long bonds, which is exhibited most clearly by the neutral form, will be partially destroyed in the protonated species in which the short double bonds become longer and the long single bonds become shorter. This effect is more pronounced toward the terminal nitrogen, so that, in the case of the protonated Schiff base, the B_3 double bond (1.396 Å) is even longer than the B_2 single bond (1.388 Å) (Tables 1 and 2). It has to be mentioned, however, that the large effect of the protonation on the bond alternation of the molecule could be partly related to the overestimation of the π-electron delocalization when using DFT calculations and such bond length inversion of a single bond and a double bond has not been observed in calculations using a multireference wave function.

The bond length of the C═N group in the protonated Schiff base is, on the other hand, 1.332 Å which is significantly longer than the corresponding value of 1.284 Å in the unprotonated Schiff base. The weakening of the double bonds and the strengthening of the single bonds will significantly influence the rotation barriers of different single or double bonds.[49,57,61,62] This effect can be explained by the partial migration of π-electron charge to the Schiff base nitrogen, rendering the other part of the π system positive as it can be clearly observed from the pattern of charge distributions (Tables 3 and 4).

Because of the presence of a positive charge in the molecule, different mesomeric structures can be considered for the protonated Schiff base. These mesomeric structures are schematically presented in Figure 2. In the first structure (A in Figure 2) the positive charge is formally carried by the nitrogen atom and the double bonds are drawn according to the convention which is generally used to describe the retinal Schiff base. This mesomeric structure can appropriately describe the planar, cis or trans, conformers of the protonated Schiff base. Other mesomeric structures (B−G) can be obtained by shifting the π electrons of the Schiff base double bond (C═N) to the nitrogen atom. This leaves the positive charge on the other part of the molecule, namely the carbon containing moiety (C-part), where, by shifting of other double bonds, the positive charge can formally be assigned to different carbon atoms in different mesomeric structures (B−G), as depicted in Figure 2.

Isomerization barriers calculated for the protonated model Schiff base at different single or double bonds and using different levels of theory are presented in Table 5. These barriers are calculated using the energy difference between the all-trans structure and the 90°-twisted species for each bond. In each

TABLE 3: Calculated Atomic Charges ($e \times 10^{-2}$) for the All-Trans and Different 90°-Rotated Species of the Neutral Model Schiff Base[a]

	N_1	C_2	C_3	C_4	C_5	C_6	C_7	C_8	C_9	C_{10}	C_{11}	C_{12}
all-trans	−26	17	3	2	1	1	1	1	1	1	1	−1
B1-90 (R)	**−31**	**19**	2	3	1	2	1	1	1	1	7	−6
B2-90 (R)	−20	**14**	**−1**	5	0	0	0	0	0	0	7	−7
B3-90 (U)	−24	17	**4**	**−5**	5	0	0	0	0	1	6	−6
B4-90 (R)	−25	18	8	**−3**	**−4**	5	0	0	0	0	7	−7
B5-90 (U)	−25	16	5	5	**−2**	**−4**	5	1	0	1	6	−6
B6-90 (R)	−26	17	3	2	6	**−4**	**−5**	5	0	0	7	−7
B7-90 (U)	−26	16	4	1	2	5	**3**	**4**	4	1	6	−6
B8-90 (R)	−26	17	3	2	1	1	5	**−4**	**−4**	5	7	−7
B9-90 (U)	−26	16	4	1	1	1	1	5	**−4**	**−3**	9	−5
B10-90 (R)	−26	17	3	2	1	1	1	1	5	**−4**	**3**	−2

[a] The position of the rotated bond is shown as being between the atoms identified by bolded charges in adjacent columns. For the bond and atom numbering refer to the text and Figure 1. The data are derived from the calculations at the restricted B3LYP/6-31G* level of theory except when there was an unrestricted solution for description of the system. In these cases the unrestricted B3LYP/6-31G* geometries and charges are used. U and R stand for unrestricted and restricted B3LYP/6-31G* calculations, respectively.

TABLE 4: Calculated Atomic Charges ($e \times 10^{-2}$) for the All-Trans and Different 90°-rotated Species of the Protonated Model Schiff Base[a]

	N_1	C_2	C_3	C_4	C_5	C_6	C_7	C_8	C_9	C_{10}	C_{11}	C_{12}
all-trans	9	34	1	8	3	7	4	7	4	7	10	6
B1-90 (R)	**−8**	**25**	9	10	5	10	5	10	5	10	10	10
B2-90 (R)	29	**40**	**−6**	10	1	5	2	5	2	5	8	2
B3-90 (R)	−2	27	**−8**	**7**	10	11	6	11	6	11	11	12
B4-90 (R)	18	42	9	**11**	**−4**	8	1	3	1	4	8	0
B5-90 (R)	1	27	−2	8	**−5**	**8**	10	12	6	12	11	13
B6-90 (R)	15	38	4	12	9	**7**	**−4**	7	2	3	8	−1
B7-90 (U)	8	32	2	6	4	8	**1**	**4**	8	9	9	9
B8-90 (R)	12	36	3	10	4	9	9	**5**	**−3**	7	8	−1
B9-90 (U)	10	34	3	8	5	6	7	9	**4**	**1**	10	3
B10-90 (R)	10	35	2	9	3	8	4	8	8	**4**	**5**	4

[a] The position of the rotated bond is shown as being between the atoms identified by bolded charges in adjacent columns. For the bond and atom numbering refer to Figure 1. The data are derived from the calculations at the restricted B3LYP/6-31G* level of theory except when there was an unrestricted solution with lower energy. In these cases the unrestricted B3LYP/6-31G* charges are reported. U and R stand for unrestricted and restricted B3LYP/6-31G* calculations, respectively.

case the geometry of the molecule is fully optimized except for the constrains imposed for keeping the molecule at 90°-twisted conformation. In the case of the protonated Schiff base most of the 90°-twisted structures as well as the all-trans conformer are properly described by the spin-restricted B3LYP calculations, and repeating the calculations using UB3LYP does not lead to a lower energy solution for the electronic configuration of the system.

As shown by Figure 2, for the mesomeric structures B−G in the N-part of the molecule (depending on the position of the positive charge in the main chain) a number of the double bonds are converted to single bonds and vice versa. One of the consequences of this picture is that lower barriers to the rotation at the conventional double bonds are predicted in the protonated Schiff base as compared to the unprotonated species. This has clearly been described for the conjugated Schiff base structures in previous studies.[15,49,62] Another point which may be concluded from the mesomeric structures depicted in Figure 2 is that depending on the weight of the mesomeric structure drawn for the protonated Schiff base, the 90°-twisted species for isomerization of some of the double bonds in the protonated model Schiff base can be properly described by spin-restricted calculations. This is quite consistent with the results obtained in the

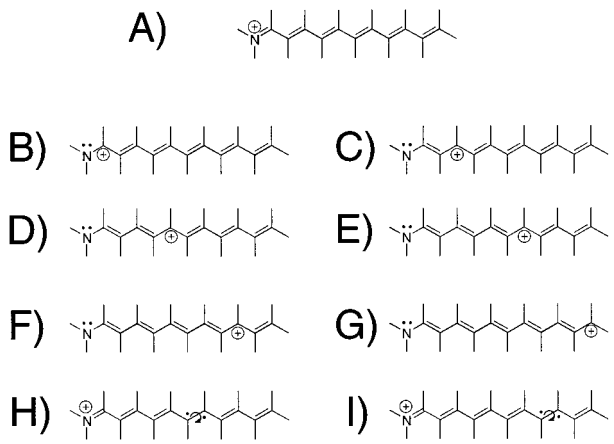

Figure 2. Mesomeric structures for the protonated Schiff base model.

present study from the calculations on the protonated Schiff base. In the protonated Schiff base the bond alternation is completely destroyed in the N-terminal moiety of the chain. Therefore, closed-shell calculations are expected to be able to appropriately predict the electronic configuration for the transition state of the rotation of the double bonds close to the Schiff base (C═N) group in the protonated species. Moving to the other end of the system (C-part) the bond alternation is gradually recovered. The bond distance of B_{11} in the protonated Schiff base model is 1.349 Å which is quite comparable to the corresponding value in the neutral Schiff base (1.345 Å). Therefore, since the rotation of a double bond in this region can be considered as a homolytic bond break, for the appropriate description of the transition state of the rotation of the double bonds in the C-part of the molecule, spin-unrestricted calculation should be used.

The results of the calculations show that, for the 90°-twisted species of the double bond isomerizations in the protonated model Schiff base, in most cases, spin-unrestricted B3LYP collapses into the spin-restricted B3LYP solution and leads to the same geometries and energies. Therefore, as it can also be observed in Table 5, the calculated barriers are the same for both closed-shell and open-shell approaches for the double bond B_1, B_3, and B_5 rotations. As we get closer to the other end of the polyene chain, however, the bond alternation is more pronounced. The double bonds located in this region, B_7 and B_9, have more double bond character than other double bonds in the protonated Schiff base, and therefore, their rotations can be considered as homolytic bond breaks. Therefore, the isomerizations at B_7 and B_9 double bonds cannot be properly described by the closed-shell calculations.

As it can be observed in Table 5, B3LYP and UB3LYP calculations result in different isomerization barriers for these two bonds. B3LYP/6-31G* level of theory predicts the values of 40.98 and 49.19 kcal/mole for the barriers against the rotation of B_7 and B_9, respectively. Application of the UB3LYP/6-31G* level of theory, on the other hand, results in the values of 37.28 and 39.98 kcal/mol for B_7 and B_9 isomerization barriers, respectively (Table 5). The UB3LYP calculations are able to determine more energetically favored solutions for the transition states of these two rotations, and the barriers calculated for the B_7 and B_9 rotations by this level of theory are 3.60 and 9.21 kcal/mol, respectively, less than the corresponding values in the B3LYP calculations. To appropriately describe the transition state of these rotations (B_7 and B_9), we have to consider other mesomeric structures showing the biradical character of the 90°-rotated species. Two of these mesomeric structures for the B_7 and B_9 rotations, H and I, respectively, are depicted in Figure

TABLE 5: Calculated Barriers (kcal/mol) to the Rotation of Different Dihedrals in the Protonated Model Schiff Base[a]

method	B_1	B_2	B_3	B_4	B_5	B_6	B_7	B_8	B_9	B_{10}
B3LYP/6-31G	28.46	31.69	29.88	29.03	35.25	22.97	41.13	17.35	60.39	11.40
UB3LYP/6-31G	28.46	31.69	29.88	29.03	34.50	22.97	37.33	17.35	39.15	11.40
B3LYP/6-31G*	28.76	30.43	29.46	28.30	35.08	22.50	40.98	17.03	49.19	11.24
UB3LYP/6-31G*	28.76	30.43	29.46	28.30	35.08	22.50	37.28	17.03	39.98	11.24

[a] For the bond numbering refer to Figure 1.

2. In each case, the radical can be stabilized by propagating through the conjugated chain on each side (in order to save space, these structures are not drawn). Although similar mesomeric structures to H and I in Figure 2 can also be depicted for the rotation of all of the double bonds, except for the B_7 and B_9 double bond rotations, they have small weights and, therefore, are not shown here.

In the case of single bond rotations, on the other hand, the 90°-twisted transitions are well described by spin-restricted B3LYP calculations and there is no better open-shell solution for the electronic configuration (Table 5). The isomerization barriers to the different single or double bonds along the chain are predicted to be very variable in the protonated Schiff base (Table 5) and can be significantly influenced by the proximity of the bond to the protonated Schiff base group.

Rotation around a single or a double bond breaks the conjugation between the Schiff base group (N-part) and the other part (C-part) of the polyene structure. The localization of the positive charge in the transition state for single or double bond isomerizations is, however, completely different. The rotation breaks, in both cases, the long conjugated system in two isolated smaller conjugated subsystems. In the case of single bond isomerizations, at the 90°-twisted transition state, the positive charge stays in the N-part and the other part of the molecule can be considered as an isolated neutral polyene system. At the 90°-twisted transition state of single bond isomerizations, the bond alternation in the C-part is calculated to be significantly larger than the all-trans conformer. This can clearly be seen from Tables 2 and 4, where bond distances and atomic charges are reported for all-trans and 90°-twisted structures. For all single bond isomerizations we have a very large bond alternation in the 90°-twisted structure in the C-part region where the sums of the charges are very close to zero (Table 4). The N-part of the 90°-twisted structures of single bond rotations, on the other hand, can be considered as an isolated protonated Schiff base in which the conjugation is much smaller than the all-trans conformer. For the 90°-twisted species in single bond isomerizations, the positive charge is completely localized in the N-part region (Table 4).

The picture describing double bond isomerizations is completely different. As it was mentioned before, in the case of most of the rotations around conventional double bonds, especially around those which are closer to the Schiff base (C═N) group, the 90°-twisted conformer can be appropriately described by a closed-shell picture and there is no open-shell solution for electronic configuration of the molecule. Depending on the position of the rotating bond, one or more mesomeric structures, depicted in the Figure 2, can be considered also for the 90°-rotated conformer. Therefore, on the basis of the mesomeric structures, in the case of the double bond rotations, we expect a different charge distribution and bond alternation in the 90°-twisted species for both N-part and C-part regions of the molecule as compared to the corresponding values in the all-trans conformer. The N-part of the molecule is converted to a neutral enamine structure with a more pronounced sp^3 hybridization state. Examination of the bond lengths in this part indicates that a completely different bond alternation can be found in the transition state (Table 2). Considering the N-part of the molecule, all of the conventional double bonds of the all-trans conformer (mesomeric structure A in Figure 2) are converted to single bonds in the 90°-rotated structure and all single bonds of the N-part in the planar structure can be considered as double bonds in the 90°-twisted species. In the all-trans conformer the positive charge, although being distributed along the polyene chain, is mainly located on the C_2 atom. In the 90°-twisted structures of the double bond rotations, however, the positive charge is completely transferred to the C-part of the molecule (Table 4). For the double bond isomerizations, therefore, the C-part can be considered as a polyenyl cation in the 90°-twisted structures. Very similar charge relocalizations have been reported for the conical intersection electronic structure described for other protonated conjugated Schiff base models during the isomerization of a double bond.[45,46]

Because of the localization of more positive charge in the C-part region, the bond alternation in this region is also influenced during the rotation of double bonds. Compared to the all-trans conformer less bond alternation will be obtained for the C-part region of the 90°-twisted species (Table 2).

3.2.2. Unprotonated Schiff Base. As compared to the protonated species, the model Schiff base shows significantly larger bond alternation in the neutral form. Due to the absence of any positive charge on the system only a slight perturbation of the pattern of bond alternation can be observed in this case. The bond distances calculated for different bonds of the all-trans neutral species (Table 1) demonstrate very close values to pure single or double bonds. In the case of the bonds in the region close to the nitrogen (B_2 and slightly B_3), however, one can observe a small conjugation which slightly disorders this general expression.

Regarding bond isomerizations, therefore, different bonds in neutral species can be considered either as a pure single bond which can readily isomerize or as a strong double bond which is predicted to have a relatively large isomerization barrier. In the case of the single bond rotations in the unprotonated model, therefore, the potential energy surface can properly be described by closed-shell calculations. The isomerization event of the double bonds, on the other hand, should be described by open-shell calculations which may appropriately handle the bond-breaking nature of the rotation, especially at the transition state region.

In the unprotonated species, the all-trans conformer as well as the 90°-rotated species of the single bond isomerizations can appropriately be described by the mesomeric structure A in Figure 3. In the case of the single bond rotations, no UB3LYP solution could be found for the 90°-twisted structures in the unprotonated model (Table 6). The calculated barriers for the single bond rotations in the unprotonated species are about 9.0−11.0 kcal/mol for 6-31G and 6-31G* basis sets (Table 6). The isomerization barriers to the different single bonds along the chain are predicted to be very close to each other, and in contrast to the protonated Schiff base, do not change, significantly. No

TABLE 6: Calculated Barriers (kcal/mol) to the Rotation of Different Dihedrals in the Neutral Model Schiff Base[a]

method	B_1	B_2	B_3	B_4	B_5	B_6	B_7	B_8	B_9	B_{10}
B3LYP/6-31G	37.20	11.01	60.59	10.93	56.00	11.31	55.78	10.88	59.57	9.15
UB3LYP/6-31G	37.20	11.01	37.41	10.93	34.06	11.31	33.67	10.88	35.97	9.15
B3LYP/6-31G*	38.95	10.43	60.73	10.69	56.03	11.14	55.73	10.74	59.48	9.05
UB3LYP/6-31G*	38.94	10.43	37.90	10.69	34.37	11.14	33.89	10.74	36.12	9.05

[a] For the bond numbering refer to Figure 1.

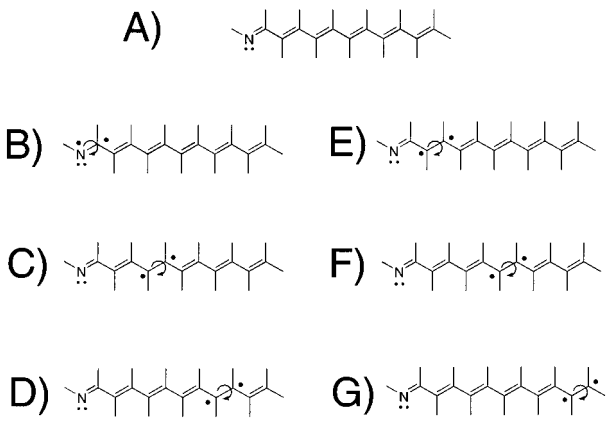

Figure 3. Mesomeric structures for the neutral Schiff base model.

significant changes can be recognized in the atomic charges of the transition state species of single bond rotations as compared to the ones in the planar conformer (Table 3). The examination of the bond distances of the conjugated system (Table 1) shows that, except for the rotating bond which becomes longer in the 90°-rotated species, there are only slight increases in the bond alternation, especially next to the rotating bond, on both C-part and N-part sides. During the rotation of the single bonds, the rupture of the conjugated system in the 90°-rotated species increases the bond alternation for both the C-part and N-part sides, respectively.

In the case of double bond isomerizations, on the other hand, depending on the location of the rotating double bond, the 90°-twisted transition state can be better described by the other mesomeric structures (B−G) depicted in Figure 3. For the double bond rotations, the transition states cannot be properly described by the application of the spin-restricted calculations. Because of the absence of any formal positive charge on the Schiff base group, the bond alternation is significantly larger in the neutral species, as compared to the one in protonated form. Therefore, rotation around a double bond breaks the π bond of the rotating double bond and results in biradical species at the 90°-twisted conformer. The radicals happening on either sides of the rotating bond are stabilized, to some extent, by the remainder of the conjugated π system in both the C-part and N-part regions. A number of possible mesomeric structures which can be used to describe the 90°-rotated species for each rotation are presented in Figure 3.

The isomerization barriers for the unprotonated model are shown in Table 6. Compared to the other double bonds, the C═N bond has a relatively lower isomerization barrier (about 38.0 kcal/mol). The isomerization barriers of the other double bonds are predicted to be too high within the spin-restricted B3LYP calculations. The rotation barriers of 55.0−60.0 kcal/mol obtained by the B3LYP method will be reduced to about 34.0−38.0 kcal/mol in the spin-unrestricted calculations (Table 6). As compared to the protonated Schiff base, the calculated isomerization barriers for double bonds in the neutral species are also relatively invariable and do not change along the chain.

In the case of the double bond rotations, the rotating bond becomes much longer and converts to a single bond at the transition state (Table 1). As compared to the values of 1.3559−1.3612 Å obtained for the B_3, B_5, B_7, and B_9 double bonds of the all-trans conformer, the length of the rotating bond is about 1.4720−1.4760 Å in the corresponding 90°-twisted isomers. In the case of the double bond rotations, the bond alternation of both the N-part and C-part sides are more significantly perturbed in the 90°-twisted species of the double bond rotations (Table 1). This can be related to the stabilizing effect of the π-system on the radicals produced at the 90°-twisted conformers.

The atomic charges are also influenced by the rotation of the double bonds. The calculated atomic charges of the 90°-rotated species, however, are within less than 0.1 e different from the atomic charges in the all-trans conformer (Table 3).

TABLE 7: Calculated Proton Affinities (kcal/mol) for the All-Trans and Different 90°-Rotated Species of the Model Schiff Base[a]

method	B3LYP/ 6-31G	UB3LYP/ 6-31G	B3LYP/ 6-31G*	UB3LYP/ 6-31G*
all-trans	264.52	264.52	257.65	257.65
B1-90	273.26	273.26	267.84	267.84
B2-90	243.84	243.84	237.65	237.65
B3-90	295.22	272.04	288.92	266.12
B4-90	246.42	246.42	240.04	240.04
B5-90	285.27	264.08	278.60	256.94
B6-90	252.86	252.86	246.30	246.29
B7-90	279.17	260.86	272.41	254.26
B8-90	258.05	258.05	251.35	251.35
B9-90	263.71	261.35	267.94	254.79
B10-90	262.27	262.27	255.45	255.45

[a] For the bond numbering refer to Figure 1.

3.3. Proton Affinity. DFT has been reported to be very reliable in calculating PA and in reproducing the experimental results within a few kcal/mol.[63] The results of DFT calculations show a significant improvement over Hartree−Fock results, and it has also been reported that MP2 and MP4 do not significantly improve the DFT-calculated PA values.[51] This is also evident from comparison of the calculated PA values of methylenimine at the MP3/6-31G* (214.2 kcal/mol, ref 64) and Becke3LYP/6-31G* (216.2 kcal/mol, ref 49) levels of theory.

To study the potential effect of the rotation of different bonds on the pK_a of the retinal Schiff base, we have also calculated the gas-phase proton affinity (PA) of our model Schiff base in 90°-twisted conformers as well as in the all-trans conformer. The PA values calculated using B3LYP or UB3LYP methods and different basis sets are presented in Table 7. The PA values calculated at the UB3LYP/6-31G* level of theory are also graphically depicted in Figure 4. As compared to the UB3LYP/6-31G results, application of the larger basis set, 6-31G*, causes a systematic shift of 6.0−7.0 kcal/mol in the PA values for both all-trans and 90°-rotated structures (Table 7). Therefore, the application of a larger basis set does not influence the conclusions about the isomerization effect on the pK_a of the Schiff base in the present study. This observation has also been previously reported in comparative studies of the analogous Schiff base structures.[49,50] In those studies it was found that application of 6-31G* or 6-31G** basis sets, although resulting in different absolute PA values, caused a constant systematic

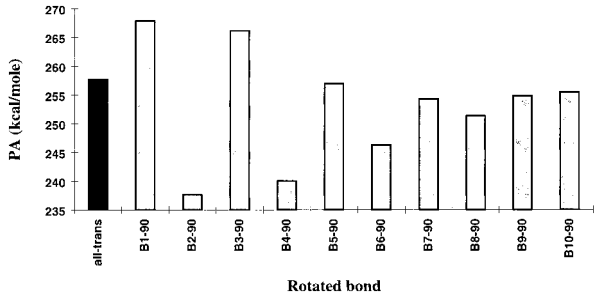

Figure 4. Comparison of the calculated proton affinity for all-trans and 90°-rotated species of the model Schiff base. For the bond numbering refer to Figure 1. The data are calculated on the basis of the calculations at the restricted B3LYP/6-31G* level of theory except when there was an unrestricted B3LYP solution with lower energy for the protonated and/or neutral species. In these cases the energetically more favorable unrestricted B3LYP/6-31G* energies of the protonated and/or neutral species were used.

shift of PA and could not influence the PA differences calculated for different molecules. The application of the larger basis set, 6-31G**, resulted in the higher PA values (about 2.0 kcal/mol) calculated for the conjugated Schiff base structures,[49] while in the present study larger basis set resulted in the lower absolute PA values.

In a recent paper we showed that, in a small conjugated model Schiff base, isomerization can significantly influence the calculated PA of the system. More interestingly the rotation of a double bond was shown to have a completely different effect on the PA as compared with the rotation of a single bond.[49] Due to the short length of the model Schiff base studied in that study,[49] however, to have a more reliable and more quantitative conclusion, we decided to study here how the isomerization may influence the PA in a model Schiff base with six conjugated double bonds. As it can be seen from the results presented in Table 7 and Figure 4, the rotation of a double bond increases the PA of the Schiff base. This effect is much more significant for the double bonds close to the Schiff base group (C═N), and the increase of the PA due to the double bond rotations is most significantly observed in the case of the B_1, B_3, and B_5 rotations, respectively.

At the 90°-rotated species of the B_3 rotation, the PA is calculated to be 266.12 kcal/mol, which is about 8.50 kcal/mol larger than the corresponding value in the all-trans conformer (257.65 kcal/mol). This PA difference corresponds to a pK_a change of about 6.0 pH unit. However, since it is unlikely that the retinal chromophore adopts a 90°-twisted structure in the protein environment, the PA changes calculated here can only be qualitatively used to estimate the effect of a twist on the pK_a of the retinal Schiff base. It is worthwhile to have a closer and more detailed look at the shape of the potential energy surface of this rotation in a large conjugated system like the one used in the present study. In this way, one may estimate the PA change of the retinal Schiff base in its twisted conformers. These calculations are being performed in this laboratory.

The lowering effect of the protonation on the double bond isomerization barriers, which has been experimentally shown[65] (particularly for C═N and C_{13}═C_{14} double bonds of the retinal Schiff base, it is shown that the ground-state rotation can only happen in the protonated form), can be used as an energetic basis for explaining why the PA increases during the rotation of a double bond. As mentioned before, although the absolute values for the isomerization barriers calculated using single-reference DFT calculations in the present work are different from the calculations applying multireference wave functions, the changes in the PA of the system show the same trends in DFT and CAS−SCF calculations.

The calculated increase of the PA at the 90°-rotated species of the B_3 rotation can be rationalized by the inspection of the atomic charges (Table 4) and the bond alternation (Table 2) of the protonated polyene structure in the 90°-rotated species, as compared with the corresponding values of the planar conformer. The rotation of a double bond separates the conjugated system into two segments which will substantially differ from their electronic state in the all-trans conformer. At the 90°-rotated conformer, we have a more negative (less positive in the case of protonated species) N-part at one side and a more positive C-part on the other side (Table 4). In this way, during the rotation of the double bonds, the protonated Schiff base group leaves the positive charge on the C-part of the molecule and will be converted to a neutral amine group which is known to have a much larger pK_a than a protonated Schiff base group. For the B_3 rotation, the total charge located in the Schiff base-containing region (N_1, C_2, and C_3) of the protonated species at the transition state is only 0.17 e which is significantly smaller than the corresponding value of 0.44 e in the all-trans conformer (Table 4). For the discussion of bond alternation changes we refer to the previous sections (isomerization barriers in the protonated and neutral species).

The single bond rotations, on the other hand, have completely different influences on the calculated PA of the Schiff base. At a torsion angle of 90° of a single bond, the molecule can be considered as two mutually isolated π-electronic systems. In this case, the rotation of a single bond shortens the length of the π-electronic system conjugated to the protonated Schiff base group and, therefore, the PA is predicted to decrease during the single bond isomerizations. The C-part of the conjugated system at the 90°-twisted transition state of the single bond rotations can be best described as an isolated neutral polyene chain with a larger bond alternation as compared to the all-trans conformer. Therefore, in agreement with the previously reported results,[15,49] we conclude that any deviation of the single bonds from the planar structure of the retinal Schiff base decreases the pK_a of the system.

According to the available crystallographic data for retinal[66,67] and *N*-methyl-N-phenylimine retinal Schiff base,[58] the retinal polyene molecule has a planar structure in the crystal form. The large steric hindrance of the substituted methyl group on the polyene chain is, to some extent, compensated by the adoption of a banana-shaped structure by the molecule. In the protein environment, however, the steric interaction of the binding pocket with the chromophore influences the structure adopted by the chromophore. There are experimental and theoretical studies which propose a twisted structure of the retinal Schiff base in the bR protein environment. The biphasic nature of the CD spectrum of the retinal Schiff base in bR has been explained on the basis of adoption of a twisted structure by the chromophore.[68] In a very recent paper, more evidence for nonplanarity of the retinal Schiff base structure in the protein environment has been reported after the analysis of the optical rotation of the second harmonic radiation from retinal in bR monomers in Langmuir−Blodgett film.[69] Polarized infrared spectroscopy studies also suggest the existence of distortions around different dihedral angles along the retinal chain.[70,71]

There are experimental studies which demonstrate the ground-state rotation of the C═N and C_{13}═C_{14} double bonds in different analogues of the protonated retinal Schiff base.[65,72] In these studies C═N and C_{13}═C_{14} isomerization have been monitored

using NMR techniques. In the present work, we found that the barriers against the rotation of C═N and C_{13}═C_{14} double bonds of a model Schiff base are lower than the other double bonds. Although, on the basis of the calculated bond alternation, DFT seems to predict lower barriers for the rotation of double bonds than CAS−SCF, the computed barriers (about 30 kcal/mol in the present study) are still too high to explain the ground-state isomerization of the chromophore around these two double bonds in room temperature.

With regard to the high barriers calculated for the rotation of the double bonds, as compared to the experimental observations, we are not aware of any reported methodological problem. The addition of the methyl groups to the applied model can improve (decrease) the rotational barriers. Preliminary results of our calculations show that, in such a methylated model, the barrier against the B_1 and B_3 rotations will be decreased about a few kcal/mol. This effect can be related to the steric effect of the substituted methyl groups, which is more significant in the planar structure (compared to the twisted one), and the stabilization effect of the methyl groups on the relocalized positive charge of the C-part of the 90°-twisted conformer.

However, the decreasing effect of the methyl groups on the isomerization barriers is not large enough to explain the room-temperature rotation of the double bonds. We think that the strong polarization effects of the environment (solvent or protein matrix), which are absent in our calculations, are important factors responsible for such differences. For planar structures, for example, we showed that the application of an implicit solvent model significantly influences the energies and the structures of the conjugated Schiff base models, as compared to the gas-phase calculations.[18] Therefore, the application of a solvent model in the calculations may have significant effects on the calculated isomerization barriers.

The isomerization barriers of the B_1 and B_3 double bond should be low enough to let the chromophore do ground-state isomerization in bR. It has been reported that the protonated retinal Schiff base chromophore performs ground-state rotation around the C═N and C_{13}═C_{14} double bonds in the protein environment. These ground-state isomerization events happen during the last step of the bR photocycle as well as in the dark adaptation of the pigment and require a low barrier to the C═N and C_{13}═C_{14} double bond rotations. bR contains in its dark adapted form 13-*cis*- and *all-trans*-retinal iminium salt chromophores in thermal equilibrium. Therefore, it is quite possible that the retinal structure acquires a twisted structure at the C_{15}═N_{16} and/or C_{13}═C_{14} double bonds in the protein environment. If this happens, according to the present results, a part of the pK_a increase of the retinal Schiff base in bR, as compared to the solution form of the chromophore, can be related to the protein-induced twists in the C═N and C_{13}═C_{14} double bonds. With this respect, the potential importance of the methyl substitution at C_{13} and its steric interaction with the protein environment can also be discussed.

4. Conclusions

We have studied the barriers to the rotation of different bonds in a conjugated Schiff base molecule in both protonated and unprotonated forms. The single bond rotations in both protonated and neutral species can be well described by the closed-shell calculations. In the protonated species the double bonds in the region close to the Schiff base group which are important for the biological role of the retinal Schiff base have less double bond character and, therefore, their rotation can be properly described by the closed-shell calculations, as well. Because of the biradical character of the transition states, other double bond rotations in the protonated Schiff base, as well as all double bond rotations in the unprotonated Schiff base, however, should be considered using spin-unrestricted calculations. The isomerization barriers to the different single or double bonds along the chain are predicted to be very variable in the protonated Schiff base and can be significantly influenced by the proximity of the bond to the protonated Schiff base group. The isomerization barriers calculated for the single and double bonds in the neutral species, on the other hand, do not change significantly for different bonds along the chain.

The results clearly show that protonation of the nitrogen atom in the Schiff base (C═N) group has a profound effect on the barriers to the rotation around different bonds in the system. For the 90°-twisted transition states, completely different mesomeric structures for both single and double bond rotations of protonated and neutral species are predicted. The rotations around the Schiff base group (C═N) and the double bond next to the Schiff base in the protonated species (corresponding to the rotating bond during the photoisomerization of the retinal Schiff base in the bR) have the lowest rotational barriers among the double bonds. In the neutral species, however, higher barriers to these rotations are predicted. Therefore, in agreement with the accepted scheme of the bR photocycle and the dark adaptation of the pigment and the experimental results, the ground-state isomerizations of the chromophore around the C_{13}═C_{14} bond may only happen when the Schiff base group is in the protonated form. Protonation seems to be essential for the chromophore to be able to overcome the high barrier which exists against the rotation of this conventionally double bond.

The PA of the system decreases upon isomerization around the single bonds, while ground-state rotation around the double bonds, particularly in the region close to the Schiff base group, significantly increases the calculated values of PA. Because of the known small barriers against the rotation of the C_{15}═N_{16} and C_{13}═C_{14} double bonds in the retinal Schiff base and steric interactions of the chromophore with the protein environment, a twisted structure can be proposed for the polyene in its binding pocket. In this case, according to the results of the present work, the pK_a increase of the retinal Schiff base in bR can be partially related to such a twisted structure.

References and Notes

(1) Oesterhelt, D.; Tittor, J.; Bamberg, E. *J. Bioenerg. Biomembr.* **1992**, *24*, 181.
(2) Mathies, R. A.; Lin, S. W.; Ames, J. B.; Pollard, W. T. *Annu. Rev. Biophys. Biophys. Chem.* **1991**, *20*, 491.
(3) Lanyi, J. K. *Biochim. Biophys. Acta* **1993**, *1183*, 241.
(4) Rotschild, K. J. *J. Bioenerg. Biomembr.* **1992**, *24*, 147.
(5) Krebs, M. P.; Khorana, H. J. *J. Bacteriol.* **1993**, *175*, 1555.
(6) DuPuis, P.; Harosi, I.; Sandorfy, C.; Leclerq, J.; Vocelle, D. *Rev. Can. Biol.* **1980**, *39*, 247.
(7) Hildebrandt, P.; Stockburger, M. *Biochemistry* **1984**, *23*, 5539.
(8) de Groot, H.; Harbison, G.; Herzfeld, J.; Griffin, R. *Biochemistry* **1989**, *28*, 3346.
(9) Pebay-Peyroula, E.; Rummel, G.; Rosenbusch, J. P.; Landau, E. M. *Science* **1997**, *277*, 1676.
(10) Lueke, H.; Richter, H. T.; Lanyi, J. K. *Science* **1998**, *280*, 1934.
(11) Gat, Y.; Sheves, M. *J. Am. Chem. Soc.* **1993**, *115*, 3772.
(12) Nina, M.; Roux, B.; Smith, J. C. *Biophys. J.* **1995**, *68*, 25.
(13) Roux, B.; Nina, M.; Pomes, R.; Smith, J. C. *Biophys. J.* **1996**, *71*, 670.
(14) Orlandi, G.; Schulten, K. *Chem. Phys. Lett* **1979**, *64*, 370.
(15) Tavan, P.; Schulten, K.; Oesterhelt, D. *Biophys. J.* **1985**, *47*, 415.
(16) Warshel, A. *Photochem. Photobiol.* **1979**, *30*, 285.
(17) Warshel, A. *Methods Enzymol.* **1986**, *127*, 578.
(18) Tajkhorshid, E.; Suai, S. *Chem. Phys. Lett.* **1999**, *299*, 457.
(19) Scheiner, S.; Hillenbrand, E. A. *Proc. Natl. Acad. Sci. U.S.A.* **1985**, *82*, 2741.
(20) Scheiner, S.; Duan, X. *Biophys. J.* **1991**, *60*, 874.

(21) Baasov, T.; Sheves, M. *Biochemistry* **1986**, *25*, 5249.
(22) Rousso, I.; Friedman, N.; Sheves, M.; Ottolenghi, M. *Biochemistry* **1995**, *34*, 12059.
(23) Druckman, S.; Ottolenghi, M.; Pande, A.; Pande, J.; Callender, R. H. *Biochemistry* **1982**, *21*, 4953.
(24) Sheves, M.; Friedman, N.; Albeck, A.; Ottolenghi, M. *Proc. Natl. Acad. Sci. U.S.A.* **1986**, *83*, 3262.
(25) Tajkhorshid, E.; Suhai, S. *Theor. Chem. Acc.* **1999**, *101*, 180. (published online; Dec 10, 1998; DOI 10.1007/s00214980m120).
(26) Logunov, S. L.; El-Sayed, M. A.; Lanyi, J. K. *Biophys. J.* **1996**, *70*, 2875.
(27) Song, L.; El-Sayed, M. A.; Lanyi, J. K. *J. Phys. Chem.* **1996**, *100*, 10479.
(28) Logunov, S. L.; El-Sayed, M. A.; Song, L.; Lanyi, J. K. *J. Phys. Chem.* **1996**, *100*, 2391.
(29) Song, L.; El-Sayed, M. A.; Lanyi, J. K. *Science* **1993**, *261*, 891.
(30) Logunov, S. L.; Song, L.; El-Sayed, M. A. *J. Phys. Chem.* **1996**, *100*, 18586.
(31) Bifone, A.; de Groot, H. J. M.; Buda, F. *Chem. Phys. Lett.* **1996**, *248*, 165.
(32) Warshel, A.; Chu, Z. T.; Hwang, J. K. *Chem. Phys.* **1991**, *158*, 303.
(33) Nonella, M.; Windemuth, A.; Schulten, K. *J. Photochem. Photobiol.* **1991**, *54*, 937.
(34) Zhou, F.; Windemuth, A.; Schulten, K. *Biochemistry* **1993**, *32*, 2291.
(35) Humphrey, W.; Lugonov, I.; Schulten, K.; Sheves, M. *Biochemistry* **1994**, *33*, 3668.
(36) Humphrey, W.; Xu, D.; Sheves, M.; Schulten, K. *J. Phys. Chem.* **1995**, *99*, 14549.
(37) Lugonov, I.; Humphrey, W.; Schulten, K.; Sheves, M. *Biophys. J.* **1995**, *68*, 1270.
(38) Xu, D.; Sheves, M.; Schulten, K. *Biophys. J.* **1995**, *69*, 2745.
(39) Xu, D.; Martin, C.; Schulten, K. *Biophys. J.* **1996**, *70*, 453.
(40) Lugonov, I.; Schulten, K. *J. Am. Chem. Soc.* **1996**, *118*, 9727.
(41) Warshel, E. *Nature* **1976**, *260*, 679.
(42) Warshel, A. *Proc. Natl. Acad. Sci. U.S.A.* **1978**, *75*, 2558.
(43) Warshel, A.; Chu, Z. T.; Hwang, J.-K. *Chem. Phys.* **1991**, *158*, 303.
(44) Vreven, T.; Bernardi, F.; Garavelli, M.; Olivucci, M.; Robb, M. A.; Schlegel, H. B. *J. Am. Chem. Soc.* **1997**, *119*, 12687.
(45) Garavelli, M.; Celani, P.; Bernardi, F.; Robb, M. A.; Olivucci, M. J. *J. Am. Chem. Soc.* **1997**, *119*, 6891.
(46) Garavelli, M.; Vreven, T.; Celani, P.; Bernardi, F.; Robb, M. A.; Olivucci, M. *J. Am. Chem. Soc.* **1998**, *120*, 1285.
(47) *Insight II User Guide*, Oct 1995; Biosym/MSI: San Diego, CA, 1995.
(48) Frisch, M. J.; Trucks, G. W.; Schlegel, H. B.; Gill, P. M. W.; Johnson, B. G.; Robb, M. A., Cheeseman, J. R.; Keith, T.; Peterson, G. A.; Oritz, J. V.; Foresman, J. B.; Cioslowski, J.; Stefanov, B. B.; Nanayakkara, A.; Challacombe, M.; Peng, C. Y.; Ayala, P. Y.; Chen, W.; Wong, M. W.; Andres, J. L.; Replogle, E. S.; Gomperts, R.; Martin, R. L.; Fox, D. J.; Binkley, J. S.; Defrees, D. J.; Baker, J.; Stewart, J. P.; Head-Gordon, M.; Gonzales, C.; Pople, J. A. *Gaussian 94*, revision C.3; Gaussian, Inc.: Pittsburgh, PA, 1985.
(49) Tajkhorshid, E.; Paizs, B.; Suhai, S. *J. Phys. Chem. B* **1997**, *101*, 8021.
(50) Tajkhorshid, E.; Suhai, S. *J. Phys. Chem.*, submitted for publication.
(51) de Lera, A. R.; Iglesias, B.; Rodriguez, J.; Alvarez, R.; Lopez, S.; Villanueva, X.; Padros, E. J. *J. Am. Chem. Soc.* **1995**, *117*, 8220.
(52) Wang, Q.; Kochendoerfer, G. G.; Schoenlein, R. W.; Verdegem, P. J. E.; Lugtenburg, J.; Mathies, R. A.; Shark, C. V. *J. Phys. Chem.* **1996**, *100*, 17388.
(53) Kochendoerfer, G. G.; Verdegen, P. J. E.; van der Hoef, I.; Lugtenburg, J.; Mathies, R. A. *Biochemistry* **1996**, *35*, 16230.
(54) Schreckenbach, T.; Walckhoff, B.; Oesterhelt, D. *Biochemistry* **1987**, *17*, 5353.
(55) Harbison, S.; Smith, S.; Pardoen, J.; Courtin, J.; Lugtenburg, J.; Herzfeld, J.; Mathies, R.; Griffin, R. *Biochemistry* **1985**, *24*, 6955.
(56) Van der Steen, R.; Biesheuvel, P.; Mathies, R.; Lugtenburg, J. *J. Am. Chem. Soc.* **1986**, *108*, 6410.
(57) Froese, R. D. J.; Komaromi, I.; Byun, K. S.; Morokuma, K. *Chem. Phys. Lett.* **1997**, 335.
(58) Santarsiero, B. D.; James, M. N. G.; Mahendran, M.; Childs, R. F. *J. Am. Chem. Soc.* **1990**, *112*, 9416.
(59) Paizs, B.; Tajkhorshid, E.; Suhai, S. *J. Phys. Chem. B* **1999**, in press.
(60) Bernardi, F.; Garvavelli, M.; Olivucci, M.; Robb, M. A. *Mol. Phys.* **1997**, *92*, 359.
(61) Warshel, A.; Deakyne, C. *Chem. Phys. Lett.* **1978**, *55*, 459.
(62) Warshel, A.; Ottolenghi, M. *Photochem. Photobiol.* **1979**, *30*, 291.
(63) Fitzgerald, G.; Andzelm, J. *J. Phys. Chem.* **1991**, *95*, 10531.
(64) Del Bene, J. E. *J. Comput. Chem.* **1984**, *5*, 381.
(65) Sheves, M.; Baasov, T. *J. Am. Chem. Soc.* **1984**, *106*, 6840.
(66) Simmons, C. J.; Liu, R. S. H.; Denny, M.; Seff, K. *Acta Crystallogr., Sect. B* **1981**, *37*, 2197.
(67) Hamanaka, T.; Mitsui, T.; Ashida, T.; Kakudo, M. *Acta Crystallogr., Sect. B* **1972**, *28*, 214.
(68) Wu, S.; El-Sayed, M. A. *Biophys. J.* **1991**, *60*, 190.
(69) Volkov, V.; Svirko, Y. P.; Kamalov, V. F.; Song, L.; El-Sayed, M. A. *Biophys. J.* **1997**, 3164.
(70) Seibert, F. *NATO ASI Ser. C. Spectrosc. Biol. Mol.* **1984**, *139*, 347.
(71) Seibert, F.; Jaeger, F.; Weidlich, O.; Sheves, M. *Conf. Proc.: Spectrosc. Biol. Mol., Europ. Conf.* **1995**, *6*, 175−176.
(72) Albeck, A.; Livnah, N.; Gottlieb, H.; Sheves, M. *J. Am. Chem. Soc.* **1992**, *114*, 2400.